Hydrothermal Synthesis of CeO2/rGO nanocomposite and its Characterization

V. Ramanjaneyulu[1], K. Peddintaiah[1], Ch. Maneesha[1], A. Rajasekhar Babu[1]

[1] *Department of Chemical Engineering, JNTUA College of Engineering, Ananthapuramu*

**Corresponding Author E-mail: ramanjaneyulu.chem@jntua.ac.in*

ABSTRACT:

Graphene materials are remarkable catalysts for energy and sensor applications due to their special properties. In this study, CeO_2 and CeO_2/rGO NCs were prepared using a straight forward hydrothermal process that involved heating the material to 210°C for 24 hours. These composites have a cubic structure, according to the PXRD data, which indicates strong crystallinity. The obtained structure suits with the JCPDS card No. 34-0394, which has space group Fm-3m. Scanning electron microscopy, transmission electron microscopy (TEM/HRTEM), selected area electron diffraction (SAED), and energy dispersive spectroscopy (EDAX) were used to examine the morphological and structural elemental compositions. The present work projects the morphological and structural pattern of CeO_2/rGO NCs.

Keywords: CeO_2/rGO, Hydrothermal process, EDAX, PXRD, TEM/HRTEM

Introduction:

Over the past two decades, carbon-based substrates have exhibited tremendous influence over the designing of sustainable advanced materials for energy and environment applications [1,2]. In comparison with the carbon nanotubes and graphene, graphene oxide (GO) is more desirable for composite fabrication, mainly due to its 2D structure, remarkable stability, large surface area, enhanced conductivity [3,4]. In precise particular, reduced graphene oxide (rGO) is more effective in deposition of metal/metal oxides on its surface, making it more suitable for catalytic applications [5–7]. NCs of rGO with metal oxides have attracted attention due to their enhanced charge transfer at the interface, which influences the conductivity and electron transport capability of these NCs.

Several attempts have been made to develop application-driven materials such as chalcogenides and metal organic frameworks [8, 9] However, these materials require time-consuming synthetic methods and are expensive. Alternatively, deposition of different metal oxides, such as TiO_2, ZnO, and MnO_2 on rGO can yield superior NCs with extraordinary enhanced properties for electrochemical applications [10, 11]. No wonder, CeO_2/rGO NCs are likely to find applications as catalysts, sensors and electroactive materials. Kumar and Kumar have investigated the photodegradation of Methylene Blue (MB) using rGO-CeO_2 NC to successfully achieve 73% efficiency when compared to 34% efficiency as against blank CeO_2 nanoparticles on exposure to sunlight [13]. Most of the authors have attributed the excellent performance to the synergic effect between rGO and CeO_2.

In the present study, a hydrothermal approach was followed for the synthesis of CeO_2/rGO NCs with enhanced stability and electron charge transfer behaviour.

2. Experimental:

2.1. Materials and methods:

Reduced graphene oxide (purity, >99%), ammonium cerium nitrate [$(NH4)_2Ce(NO_3)_6$] (purity ≥98%), sodium hydroxide as fuel, hexadecyltrimethylammonium bromide (CTAB) (purity ≥98%) as quaternary ammonium surfactant and rest of the chemicals were purchased from Sigma-Aldrich. All the reagents were of analytical grade and were used without any further purification.

2.2. Synthesis of CeO_2/rGO NC:

A hydrothermal synthesis was used for the preparation of CeO_2/rGO NC. Initially, optimisation was carried out to identify the most favourable precursor concentrations needed to carry out the reaction to achieve a high yield. Based on the results, 0.041 g of GO was ultrasonically introduced to 25 mL of 2 M NaOH for 60 min. 6 mL of 0.05 M ammonium cerium nitrate solution was added by magnetic stirring for over 30 min. The entire content was then transferred to a 100 mL Teflon-lined stainless-steel autoclave and heated at 210 ºC for 24 hr. Subject to cooling; the obtained black precipitate was centrifuged by repeated washing with Millipore water until the supernatant liquid became clear. Finally, the sample was kept overnight in a hot air oven maintained at 60ºC.

2.3. Characterization:

Crystallographic phase studies of the synthesised samples were done by using high resolution powder X-ray diffraction studies on Thermo X'TRA X-ray diffractometer (Shimadzu 7000s) using Cu Kα radiation (λ = 1.540 Å) in the 2θ range of 5º-85º. The morphological features were studied by scanning electron microscopy with energy dispersive spectrometer and elemental mapping (FE-SEM/EDS, JSM7500F, Japan). XPS analysis was performed on a PHI 5000 X-ray photoelectron spectrometer with versa probe system using monochromatic Al Kα radiation (1486.6 eV). Raman shift was recorded at room temperature using a Raman spectrometer (MODEL T64000, Jobin Yvon Horiba, and France).

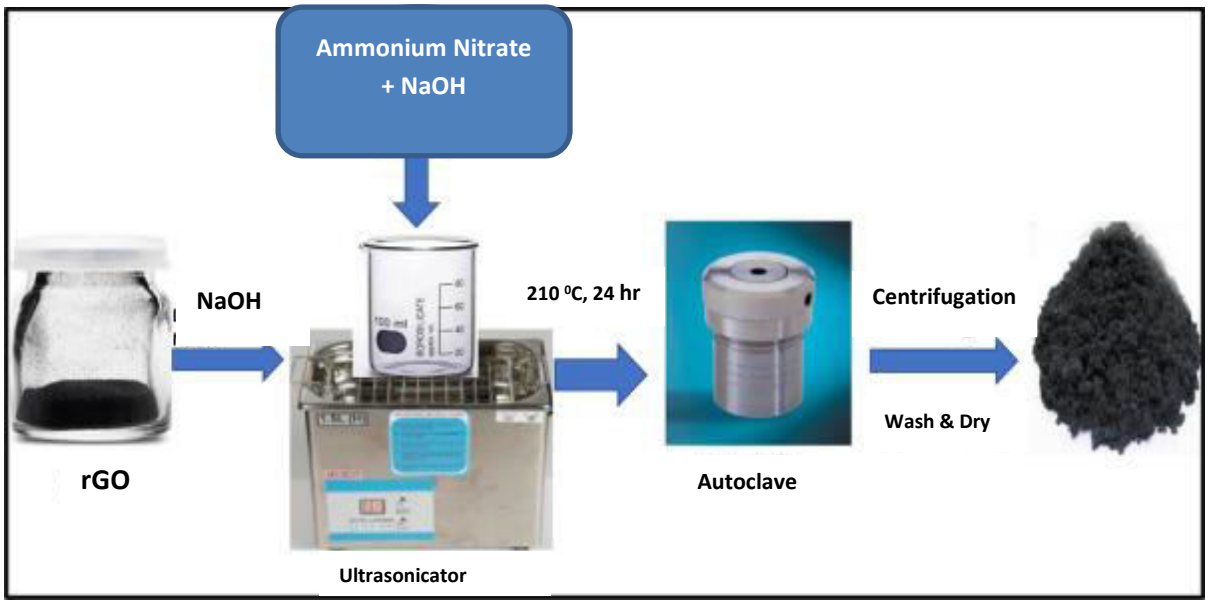

Fig.1. Schematic representation of preparation of CeO_2 and CeO_2/rGO NC.

The ambient pressure gas sorption isotherm was measured using NOVA-1000 ver.3.70 adsorption equipment. UV-Visible (UV-Vis) studies were conducted using an ELICO SL-150 spectrophotometer in the range 200 nm–800 nm using $BaSO_4$ as reference material. The cyclic voltammetry (CV) and electrochemical impedance spectroscopy (EIS) measurements were carried out using an electrochemical analyser (CHI608 potentiostat) in a tri-electrode system, comprising of Ag/AgCl (reference electrode), platinum wire (counter electrode) and the fabricated carbon paste electrode (working electrode) in 0.1N HCl solution as the electrolyte. EIS measurements in the frequency range from 1 Hz to 1 MHz were carried out at 5 mV AC amplitude.

3. Results and discussion:

3.1. pXRD analysis:

The phase purity and crystallographic studies of the synthesized NC was investigated using pXRD and Raman spectroscopy. Fig. 2(a) & (b) shows the XRD of CeO_2, CeO_2/rGO NCs. The characteristic diffraction peaks of CeO_2 microspheres with the face-centred cubic structure indicated good crystallinity (JCPDS No. 34- 0394). Sample for the pXRD analysis was prepared by grinding manually the NC using an agate mortar. It was then placed on the flat side of the sample holder, while the measurement was conducted with the scan step size of 0.02 and integration time 0.6 s per step. The diffraction peak of 10.4° is characteristic of GO [8]. Fig. 2(a) also shows the set of diffraction peaks of CeO_2 sample corresponding to fluorite type face-centred cubic structure with the cell parameters of 0.5411 nm (a=b=c); well matched with JCPDS File 34-0394. It is seen that the diffraction peak corresponding to GO at 10.4° disappeared and a prominent diffraction feature appeared at 26.3° for CeO_2/rGO NC spectra indicating the removal of oxygen functional group from GO and formation of rGO [9].

The CeO_2 crystallite size was calculated using Debye-Scherrer formula $D = K \lambda / \beta Cos\theta$ by taking the FWHM of the most intense diffraction peak. The crystallite size for pure CeO_2 and CeO_2/rGO was measured to be 6.89 nm and 6.23 nm, respectively.

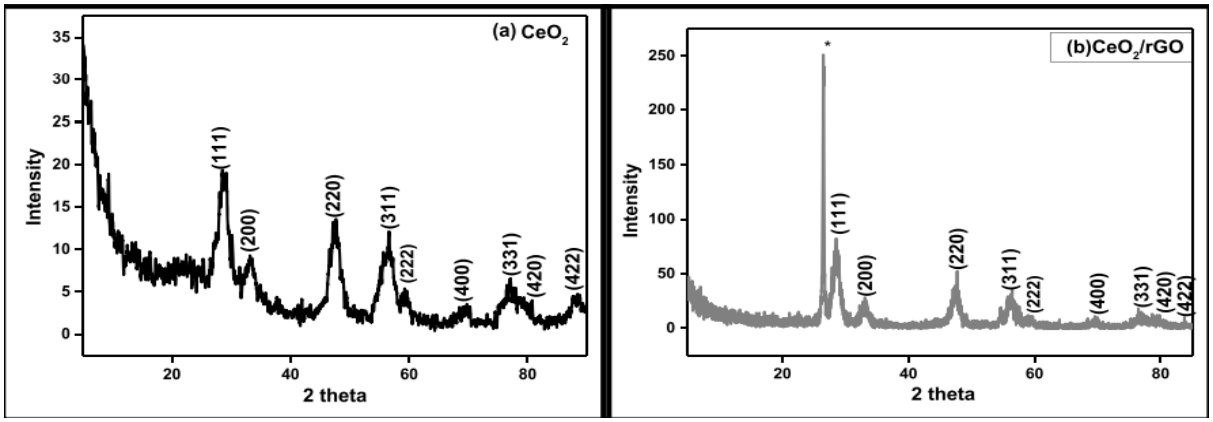

Fig.2. XRD (a & b) of CeO_2 and CeO_2/rGO NC

FESEM and EDS analysis:

The FESEM images in Fig. 3 show that the blending of rGO and CeO_2 resulted in a flake-like morphology which suggests heavy aggregation of the CeO_2 nanoparticles on the rGO sheets. The overall impact of the incorporated CeO_2 on rGO is crucial in determining the photocatalytic (in terms of quicker interaction of the catalyst with the dye molecule) and electrochemical (in terms of providing higher surface reaction sites and rapid charge transfer) activities.

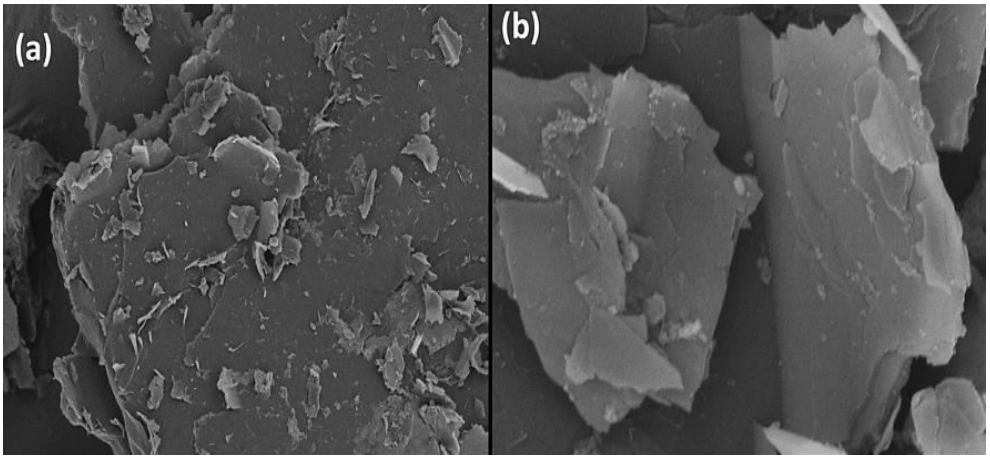

Fig.3. FESEM images of (a) CeO_2 and (b) CeO_2/rGO NCs formation

The SEM based EDS analysis carried out on a random area revealed the presence of Carbon, Cerium and Oxygen elements (Fig. 4). This was further confirmed by elemental mapping, thereby confirming the formation of CeO_2/rGO NCs.

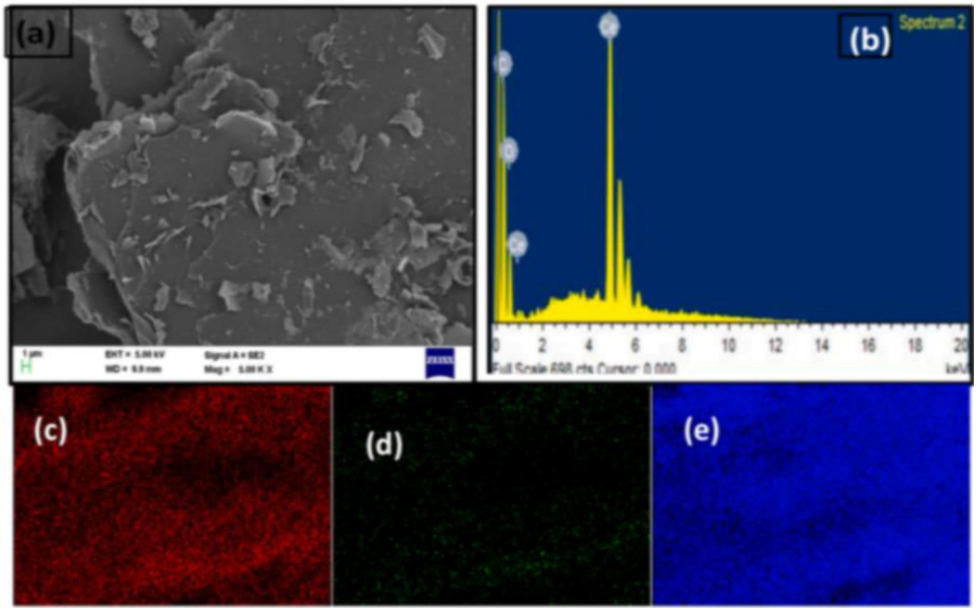

Fig. 4. (a) SEM image (b) EDAX spectra of CeO_2/rGO and the elemental ratios of (c) Carbon 20.62% (d) Oxygen 4.4%, (e) Cerium 75% in CeO_2/rGO.

3.4. XPS analysis

In order to obtain further information on the chemical composition of the synthesized sample, XPS measurements were also carried out. The obtained survey spectrum shown is evident for the presence of essential elements such as C, O and Ce (Fig. 5 (a - c)) from their corresponding photoelectron peaks C 1s, O 1s, and Ce 3d at binding energy values at 284, 532 and 884 eV, respectively [9].

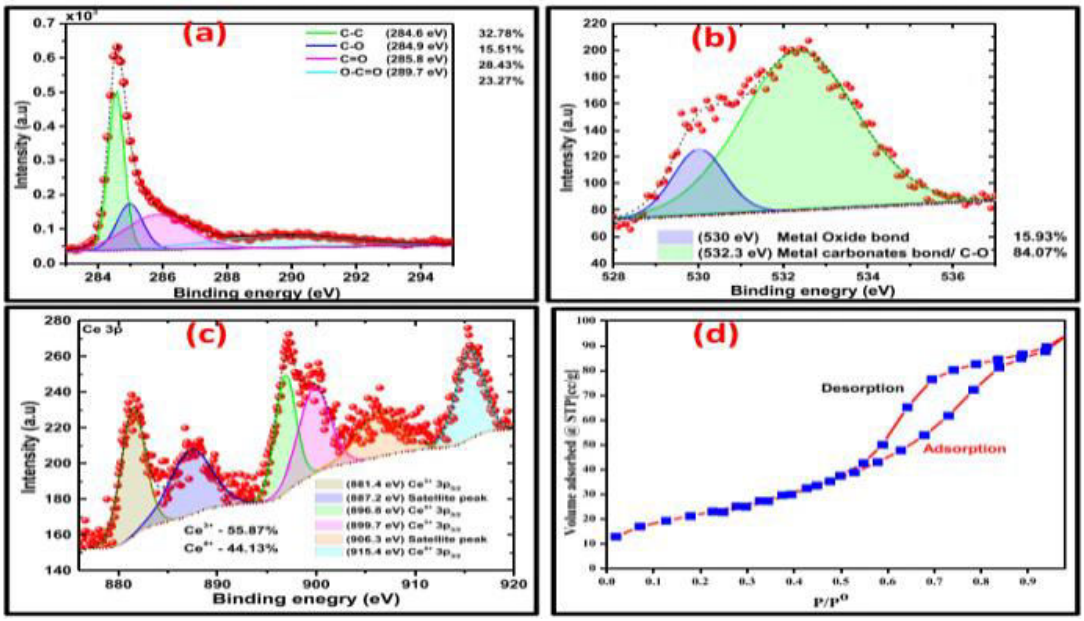

Fig. 5. XPS spectra of (a) Carbon (b) Oxygen and (c) Cerium and (d) The N_2 adsorption/desorption isotherms of CeO_2/rGO

4. Conclusion:

In conclusion, we have successfully demonstrated the synthesis of CeO_2/rGO NCs via a simple one-pot hydrothermal method. The pXRD, Raman spectroscopy and XPS provide sufficient evidence on the formation of CeO_2/rGO NC. The adsorption isotherm revealed a mesoporous nature of the NC with a low specific surface area of 100.1 m^2 /g

References:

1. J. Zhao, D. Wei, C. Zhang, Q. Shao, V. Murugadoss, Z. Guo, Q. Jiang, X. Yang, An overview of oxygen reduction electrocatalysts for rechargeable zinc-air batteries enabled by carbon and carbon composites, Eng. Sci. 15 (2021) 1–19.
2. N. Wu, W. Du, Q. Hu, S. Vupputuri, Q. Jiang, Recent development in fabrication of Co nanostructures and their carbon NCs for electromagnetic wave absorption, Eng. Sci. 13 (2021) 11–23.
3. S. Parwaiz, K. Bhunia, A. Kumar Das, M.M. Khan, D. Pradhan, Cobalt-doped ceria/ reduced graphene oxide NC as an efficient oxygen reduction reaction catalyst and supercapacitor material, J. Phys. Chem. C 121 (2017) 20165–20176.
4. R. Verma, S.K. Samdarshi, In situ decorated optimized CeO_2 on reduced graphene oxide with enhanced adsorptivity and visible light photocatalytic stability and reusability, J. Phys. Chem. C 120 (2016) 22281–22290.
5. R. Bhargava, J. Shah, S. Khan, R.K. Kotnala, Hydroelectric cell based on a cerium oxide-decorated reduced graphene oxide (CeO_2–rG) NC generates green electricity by room-temperature water splitting, Energy Fuels 34 (2020) 13067–13078.
6. Y. Wang, R.P. Liang, J.D. Qiu, Nanoceria-templated metal organic frameworks with oxidase-mimicking activity boosted by hexavalent chromium, Anal. Chem. 92 (2020) 2339–2346.
7. B. Xu, L. Xia, F. Zhou, R. Zhao, H. Chen, T. Wang, Q. Zhou, Q. Liu, G. Cui, X. Xiong, F. Gong, X. Sun, Enhancing electrocatalytic N_2 reduction to NH_3 by CeO_2 nanorod with oxygen vacancies, ACS Sustain. Chem. Eng. 7 (2019) 2889–2893.
8. S. Li, J. Fan, S. Li, H. Jin, W. Luo, Y. Ma, J. Wu, Z. Chao, N. Naik, D. Pan, Z. Guo, Synthesis of three-dimensional Mo-doped nickel sulfide mesoporous nanostructures/Ni foam composite for supercapacitor and overall water splitting, ES Energy Environ. 16 (2022) 15–25.
9. Y. Wang, Y. Liu, C. Wang, H. Liu, J. Zhang, J. Lin, J. Fan, T. Ding, J.E. Ryu, Z. Guo, Significantly enhanced ultrathin NiCo-based MOF nanosheet electrodes hybrided with Ti3C2Tx MXene for high performance asymmetric supercapacitor, Eng. Sci. 9 (2020) 50–59.